TRANSACTIONS OF THE INSTITUTE OF FLUID-FLOW MACHINERY

No. 133, 2016, 13–37

Mariusz Banaszkiewicz[a,b*], Krzysztof Dominiczak[a,b]

A methodology for online rotor stress monitoring using equivalent Green's function and steam temperature model

[a] *GE Power sp. z o.o., Stoczniowa 2, 82-300 Elbląg, Poland*
[b] *Institute of Fluid Flow Machinery, Polish Academy of Sciences, 80-231 Gdańsk, Fiszera 14, Poland*

Abstract

The requirement of high operational flexibility of utility power plants creates a need of using online systems for monitoring and control of damage of critical components, e.g., steam turbine rotors. Such systems make use of different measurements and mathematical models enabling calculation of thermal stresses and their continuous control. The paper presents key elements of the proposed system and discusses their use from the point of view of thermodynamics and heat transfer. Thermodynamic relationships, well proven in design calculations, were applied to calculate online the steam temperature at critical locations using standard turbine measurements as input signals. The model predictions were compared with operational data from a real power plant during a warm start-up and show reasonably good accuracy. The effect of variable heat transfer coefficient and material properties on thermal stresses was investigated numerically by finite element method (FEM) on a cylinder model, and a concept of equivalent Green's function was introduced to account for this variability in thermal stress model based on Duhamel's integral. This approach was shown to produce accurate results for more complicated geometries by comparing thermal stresses at rotor blade groove computed using FEM and Duhamel's integral.

Keywords: Steam turbine; Thermal stress; Green's functions; Duhamel's integral

*Corresponding Author. Email adress: mariusz.banaszkiewicz@ge.com

Nomenclature

c_0	–	isentropic velocity, m/s
c_p	–	specific heat, J/kg K
E	–	Young modulus, MPa
G	–	Green's function for stress, MPa/°C
h	–	enthalpy, kJ/kg
$\dot{m}$	–	mass flow rate, kg/s
n	–	rotational speed, rev/min
p	–	pressure, MPa
r	–	radial coordinate, m
T	–	temperature, °C
t	–	time, s
u	–	circumferential velocity, m/s
v	–	specific volume, m^3/kg
X	–	Green's function for temperature, °C/°C
y	–	valve opening, %

Greek symbols

α	–	heat transfer coefficient, W/m^2K
β	–	thermal expansion coefficient, 1/K
η	–	efficiency
λ	–	thermal conductivity, W/m K
ν	–	Poisson number
σ	–	stress, MPa

Subscripts and superscripts

CS	–	control stage
N	–	nozzle
eq	–	equivalent
T	–	throat
m	–	metal
$perm$	–	permissible
s	–	steam
$surf$	–	surface
0	–	upstream stop valves
1	–	downstream stop valves
2	–	downstream control valves
V_i	–	valve ($i = 1, 2, 3, 4$)

1 Introduction

Modern energy markets put a requirement of high operational flexibility of power plant units [1,2]. Due to this, new designed units, including steam turbines, have to fulfill a series of requirements regarding the number and rate of change of specified operation states. With regard to steam turbines, the requirements concern

the number and time of start-ups from different thermal conditions and the rate of load change. The above operation states generate elevated loads and stresses in turbine components leading to material damage due to thermomechanical fatigue [3].

The problem of thermal stress monitoring and control in steam turbines was considered already at mid-sixties [4]. In the first thermal stress control systems, steam turbine rotors were supervised using start-up probes which were thermophysical models of turbine rotors [5–7]. Thermal stresses were calculated based on measured temperature difference between the probe surface and its integral-averaged temperature. A better accuracy of stress calculation was achieved by replacing the measured average temperature with a mathematical model [8–10]. Further development of thermal stress supervision systems consisted in complete resignation from the temperature probe and modeling thermal stresses based on the standard process measurements of power units, which were a basis for calculating the characteristic temperature difference surface-mean [11]. Rusin *et al.* [12] proposed a new method of thermal stress modeling in turbine rotors employing Green's functions and Duhamel's integral, and steam temperature measurement at critical location. The Green's functions and Duhamel's integral have been for many years used for fatigue life monitoring of nuclear plants equipment by such companies like EPRI [13–15], GE [16] or EDF [17–18]. Such an approach has also been adopted for monitoring of power boilers operation by Taler *et al.* [19], and as shown by Lee *et al.* [20] can also be used for calculating stress intensity factors at transient thermal loads. Recent developments in the field are focused on the use of artificial neural networks for predicting boiler wall temperature [21] and turbine thermal stresses [22–23].

The major issue in using Green's function and Duhamel's integral method in modeling transient thermal stresses in steam turbines components is time-dependence of material physical properties and heat transfer coefficients affecting proper evaluation of Green's functions. There are known approaches assuming determination of the influence functions at constant values of these quantities [24]. The inclusion of temperature dependent physical properties proposed by Koo *et al.* [25] relies on determining the weight functions for steady-state and transient operating conditions. A more important, in most cases, variation of heat transfer coefficient can be taken into account by calculating the surface temperature using a reduced heat transfer model and employing Green's function to calculate a stress response to the step change of metal surface temperature [26]. However, numerical solution of a multidimensional heat transfer model is complicated and time-consuming, and due to this cannot be used in online calculations. A full in-

clusion of time variability of the physical properties and heat transfer coefficients proposed by Zhang *et al.* [27] relies on the solution of nonlinear heat conduction problem by using artificial parameter method and superposition rule and replacing the time-dependent heat transfer coefficient with a constant value together with a modified fluid temperature. The effectiveness of the method has been proved by an example of a three-dimensional model of a pressure vessel of nuclear reactor.

The present paper deals with the problems of modeling steam temperature and thermal stresses for online supervision of low-cycle fatigue life. A control system is proposed and its main elements are:

- thermodynamic model enabling fast calculation of steam temperature at critical location,
- thermal stress model for online calculation of rotor thermal stresses.

The models have been validated by comparing the results of numerical calculations with real turbine measurements and more accurate 3D simulations.

2 Thermal stress control system

Thermal stress control systems of steam turbine rotors are currently a commonly used measure of protecting the design fatigue life of high- and intermediate pressure turbine rotors. These systems are very important elements of turbine control and protection systems and operate in closed-loop control. A schematic diagram of turbine control system including a module responsible for thermal stress control is shown in Fig. 1. Based on turbine measurements (e.g., temperature, pressure, speed), the stress controller calculates stresses and load fraction and outputs to the turbine controller a signal of stress margin which reduces the set values of speed or load rates. The turbine controller positions, with the help of actuator, the control valve head controlling in this way the steam flow rate and temperature upstream the turbine blading. These two parameters have impact on the rotor temperature and the resulting thermal stresses.

The thermal stress controller calculates stresses at rotor critical locations on the basis of measurement signals and compares them with the permissible stresses. On the basis of these two stresses, a load fraction, LF, is calculated using the formula

$$LF = \frac{\sigma_{eq}}{\sigma_{perm}} \, . \tag{1}$$

The equivalent stress, σ_{eq}, is computed based on the measured temperature, pressure, rotational speed and using a mathematical model of temperature (if it is not

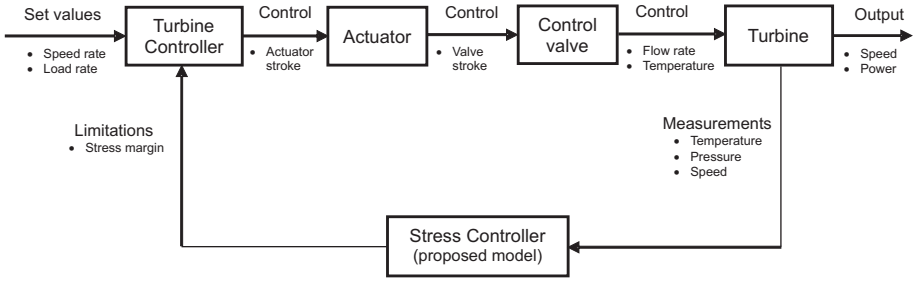

Figure 1: Schematic diagram of turbine control system with thermal stress control.

measured directly) and thermal stresses. The permissible stress, σ_{perm}, is derived from the material fatigue characteristics knowing the required number of cycles and assuming a material model.

Thus, the key elements of the considered thermal stress control system are:

- thermodynamic model allowing for steam temperature calculation at critical regions,
- thermal stress model for online stress calculation,
- relationship between elastic stress and total strain allowing for the calculation of permissible stresses for a given number of start-ups.

3 Thermodynamic model

3.1 Model formulation

In order to calculate thermal stresses at rotor critical locations, it is necessary to know the steam temperature at these locations, which is an input signal to the stress calculation algorithm. Steam temperature can be evaluated in two ways, namely:

- direct measurement of temperature at critical location using a thermocouple,
- calculation of steam temperature at critical location based on measurements at different regions and using a mathematical model.

Direct temperature measurement requires installing a measurement sensor at critical location, which is not always possible due to design restrictions. Moreover, a problem of dynamic temperature measurement error occurs due to the thermal resistance of thermocouple and thermowell, which has to be robust for mechanical integrity reasons [28]. Also heat flux variations during transients and

high-frequency unsteadiness occurring at every rotor passage with varying amplitudes originating from complex blade row interactions make the heat transfer time-dependent and accurate measurements become essential for correct thermal assessment of steam turbines [29].

A more universal way is steam temperature calculation at critical location based on a measurement at a different suitable point. For this purpose, a mathematical model is required describing steam thermodynamic process from the measurement point to the critical location. In online monitoring and control systems, the thermodynamic model should be fast, accurate and reliable, to ensure the capability of its implementation in the turbine control system and the required quality of computations. For this reason, only zero- or one-dimensional models with a minimum number of iteration loops can be considered. Modeling steam temperature is the only way of its evaluation in the areas not accessible for measurement or in turbines not equipped with the required temperature measurement.

As experience shows, the most critical region from the point of view of thermal stress is the control stage. That is why for modeling purposes we assume a steam admission system with the control stage, as shown in Fig. 2, which is typical for nozzle control.

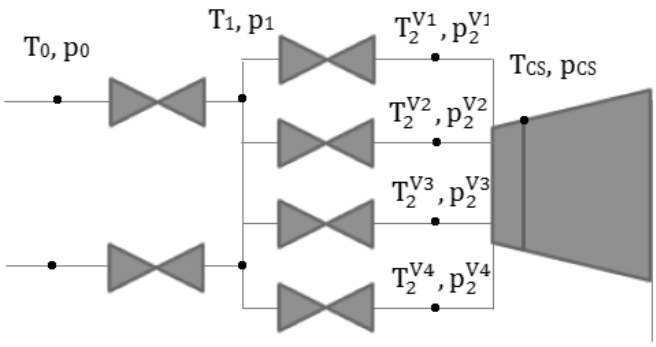

Figure 2: Steam admission system with nozzle control.

For online steam temperature calculation it is proposed to use a mathematical model employing the measurement of current opening of the control valves. The model enables online calculation of two quantities which are very important from the viewpoint of thermal loads and stresses:

- steam temperature in control stage chamber and temperatures downstream each control valve and nozzle sector for current openings,
- mass flow rates through each valve and total mass flow through the turbine.

For the considered steam admission system consisting of two stop valves and four control valves, the following measurements are used as input signals to the steam temperature model:

- live steam temperature – T_0,
- live steam pressure – p_0,
- steam pressure downstream control stage – p_{CS},
- control valves openings – y_{V1}, y_{V2}, y_{V3} and y_{V4},
- turboset rotational speed n.

The steam temperature model is based on the relations known from steam turbines theory and used in design calculations. In the proposed mathematical model these relationships are given in a consistent way with necessary simplifications and additional elements resulting from the specifity of online calculations carried out in the entire range of turbine operating conditions. In the first step, steam pressures downstream control valves and mass flow rates through each nozzle sector are calculated. One control valve cooperates in series with a nozzle sector. For such a system, the condition of equal mass flow rates can be written

$$\dot{m}_2 = \dot{m}_D \, . \tag{2}$$

The valve mass flow rate $\dot{m}_2$ is given by the relationship [30]:

$$\dot{m}_2 = 0.667 q A_T \sqrt{\frac{p_1}{v_1}} \, , \tag{3}$$

where q is a relative mass flow rate determined from the valve characteristics in a function of opening and pressure ratio, A_T – section area of valve throat, while p_1 and v_1 denote steam pressure and specific volume upstream the valve. The nozzle sector mass flow rate $\dot{m}_D$ is described by equation [31]

$$\dot{m}_N = 1.42 p_2 \left(p_0 v_0\right)^{-0.5} A_N \sqrt{-0.09 + 1.09 p_{CS}/p_2 - \left(p_{CS}/p_2\right)^2} \, , \tag{4}$$

where A_N is exit section area of nozzle sector.

A nonlinear equation with unknown p_2 is obtained from Eqs. (2)–(4) and is solved iteratively using the bisection method. Knowing the pressure p_2, we can calculate the mass flow rate from Eq. (3) or (4). Performing similar calculations for each valve, we find the appropriate pressures and mass flow rates for all valves and nozzle sectors.

In the control valves, isenthalpic process of steam throttling from upstream pressure, p_1, to downstream pressure, p_2, takes place. Assuming additionally that the enthalpy upstream the control valve is equal to the steam enthalpy upstream the stop valve, we can express steam temperature downstream the control valves as a function of steam temperature and pressures directly measured on the turbine:

$$T_2 = f(p_0,\, T_0,\, p_2)\ . \tag{5}$$

Knowing the steam temperature and pressure downstream the control valves and steam pressure downstream the control stage, we can calculate steam enthalpy using the formula known from the theory of steam turbines [31]

$$h_{CS} = \frac{h^1_{CS}\dot{m}_2^{V1} + h^2_{CS}\dot{m}_2^{V2} + h^3_{CS}\dot{m}_2^{V3} + h^4_{CS}\dot{m}_2^{V4}}{\dot{m}_2^{V1} + \dot{m}_2^{V2} + \dot{m}_2^{V3} + \dot{m}_2^{V4}}\ , \tag{6}$$

where: h^1_{CS}, h^2_{CS}, h^3_{CS}, h^4_{CS} – steam enthalpies behind each sector of the control stage.

These enthalpies depend on the circumferential efficiency, η_0, of each sector which depends on the current opening of the control valve feeding this sector. In this way, in the proposed calculation model a relationship between the control stage efficiency and current valve openings is considered. It provides a capability to take into account in online calculations the influence of valve timing on steam temperature in the control stage.

The circumferential efficiency is a function of velocity ratio u/c_0 and for on-line calculations, an individual efficiency characteristics prepared on the basis of control stage calculations using design tool is used. An example of stage efficiency characteristics is shown in Fig. 3. The results of calculations performed with the design code are presented by squares, while the continuous line represents an approximation with the function

$$\begin{aligned}\eta_o = A + B\left(\frac{u}{c_0}\right) + C\left(\frac{u}{c_0}\right)\ln\left(\frac{u}{c_0}\right) + D\left(\frac{u}{c_0}\right)^2 + \\ E\left(\frac{u}{c_0}\right)^2\ln\left(\frac{u}{c_0}\right) + F\left(\frac{u}{c_0}\right)^{2.5} + G\exp\left(-\frac{u}{c_0}\right)\end{aligned} \tag{7}$$

in which A, B, $C \ldots G$ are the coefficients of the approximation function. In this figure the values of stage efficiency are related to its maximum value.

The calculated steam enthalpy, h_{CS}, and measured pressure in the control stage, p_{CS}, allow to determine steam temperature from a thermodynamic function:

$$T_{CS} = f(p_{CS},\, h_{CS})\ . \tag{8}$$

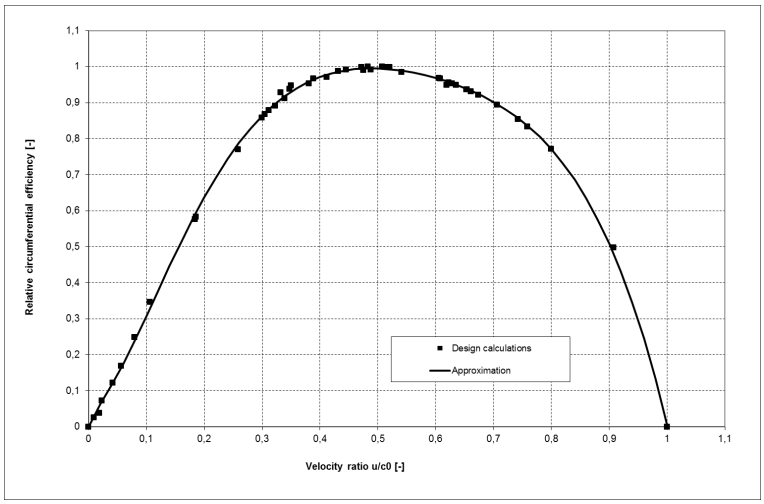

Figure 3: Dependence of control stage circumferential efficiency on velocity ratio.

3.2 Comparison with measurements

To validate the steam temperature model, measurements were carried out on a 370 MW steam turbine. A steam temperature measurement consisting of a thermowell with inserted thermocouple was installed in the control stage chamber. The temperature measurement was taken continuously and information about steam temperature was available at any instant of turbine operation. The measured temperatures were compared with the results of calculations performed using the mathematical model at various operating conditions (start-ups, shutdowns, load changes, etc.). An example of measurements and calculations is shown in Fig. 4. It presents the measured values of live steam temperature (dash line), control stage temperature (long dash line) and casing temperature (solid line) taken in the vicinity of steam temperature measurement. For the purpose of comparison also calculated steam temperature in the control stage chamber (dot line) is shown, which as it is seen from the plot, corresponds very well with the measured temperature in the entire time period. For the presented start-up the maximum temperature deviation is 17 °C, and hence the maximum relative error of calculations does not exceed 5%. Typical measurement error for the industrial temperature measurement circuit of the type used here is ±2.5 °C. Based on this it can be said that a good accuracy was achieved with this simple online model. The model calculates online steam enthalpy in the control stage and its mass flow rate, thus enabling determination of the control stage power at on-load operation.

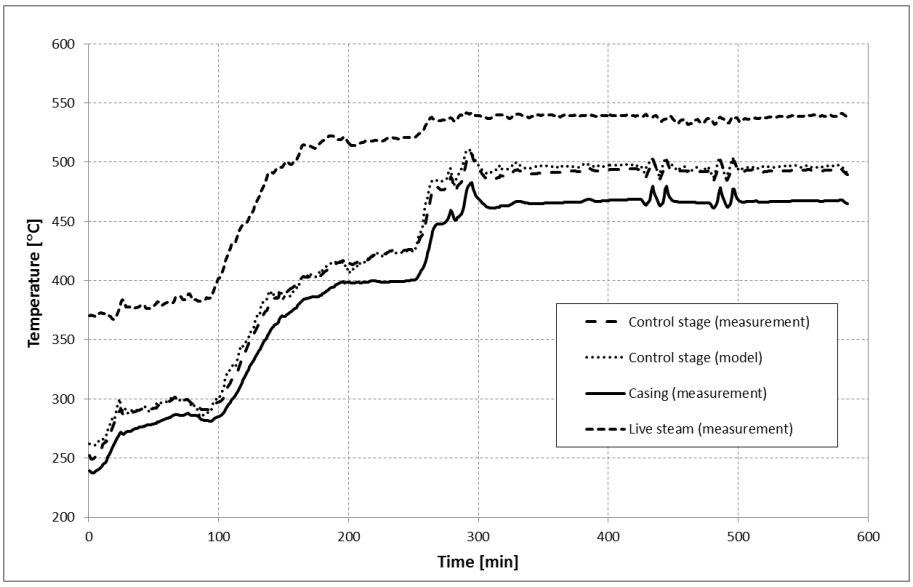

Figure 4: Measured and calculated temperature variations during warm start-up.

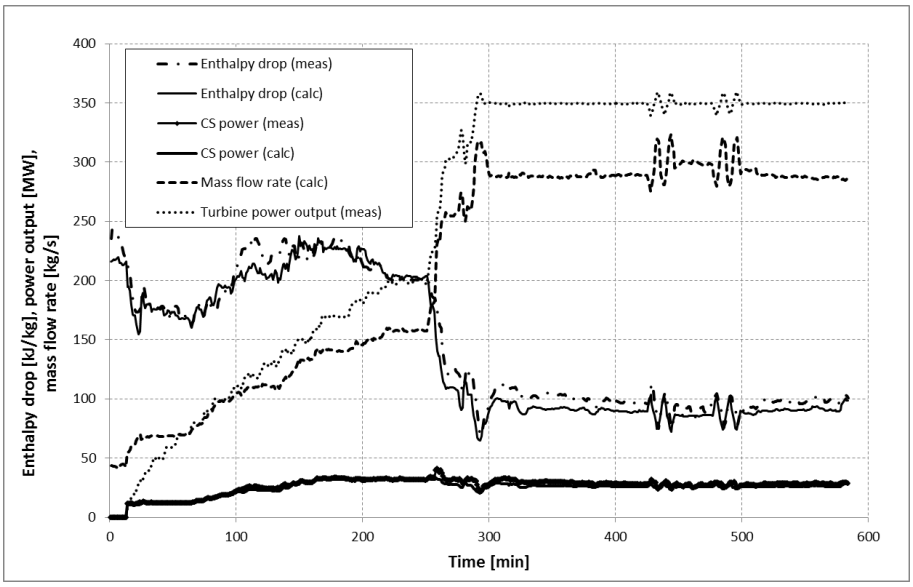

Figure 5: Mass flow rate, power and enthalpy drop variations during warm start-up.

Figure 5 presents a variation of the mass flow rate, turbine and control stage power and its enthalpy drop calculated for the analyzed warm start-up. Enthalpy drop was computed using both the calculated and measured steam temperature in the control stage. Both predictions agree very well with each other, thus the control stage power calculated based on the enthalpy drop during turbine loading can be considered as realistic.

4 Thermal stress modeling

4.1 Green's function method

It is assumed that the thermal stress model used in online calculations is based on Green's function and Duhamel's integral method. This method allows for fast calculation of thermal stresses at supervised areas for any changes of fluid temperature causing heating-up or cooling-down of an element. In steam turbine rotors a reliable and continuous measurement of the rotor surface temperature has not been possible so far, thus for online monitoring purposes the steam temperature measurement is used as a leading signal. Consequently, in heat transfer model Fourier's boundary condition is employed [32]:

$$\lambda\left(r\right)\frac{\partial T\left(r,t\right)}{\partial n}=-\alpha\left(r\right)\left(T_{s}\left(t\right)-T\left(r,t\right)\right),\quad r=R\,, \tag{9}$$

where $\lambda(r)$ is metal thermal conductivity, $T(r,\ t)$ is surface temperature, $T_s(\ t)$ denotes steam temperature, n is normal direction, $\alpha(r)$ – heat transfer coefficient, and R is the outer radius.

Assuming that steam temperature is described by Heaviside's function $H(t)$, the boundary condition Eq. (9) can be written in the form [25]

$$\lambda\left(r\right)\frac{\partial X\left(r,t\right)}{\partial n}=-\alpha\left(r\right)\left(H\left(t\right)-X\left(r,t\right)\right)\ , \tag{10}$$

where $X(r,\ t)$ is a Green's function for temperature.

Using the Green's function $X(r,\ t)$ we can calculate the metal temperature for arbitrary variation of steam temperature employing Duhamel's theorem [32]:

$$T\left(r,t\right)=\int_{0}^{t}X\left(r,t-\tau\right)\frac{\partial T_{s}\left(\tau\right)}{\partial\tau}d\tau\ . \tag{11}$$

Considering elastic stresses only it can be assumed, according to the thermo-elasticity theory, that stress distribution in an elastic body is a unique function

of temperature distribution, and in this connection the thermal stresses can be calculated using Duhamel's integral as

$$\sigma_{ij}(r,t) = \int_0^t G_{ij}(r, t-\tau) \frac{\partial T_s(\tau)}{\partial \tau} d\tau \ , \tag{12}$$

where $G_{ij}(r,\ t)$ is a Green's function for thermal stress component ij.

For simple geometries (plate, cylinder, sphere) Green's functions for temperature and stress can be determined analytically by solving one-dimensional transient heat conduction problem. In case of more complicated shapes it is necessary to use numerical methods, e.g., finite element method. Also in our case numerical integration of Eq. (12) is necessary, it is thus transformed from continuous into discrete form

$$\sigma_{ij}(r,t) = G_{s,ij}(r) T_s(t) + \sum_{t-t_d}^{t} G_{t,ij}(r, t-\tau) \Delta T_s(\tau) \ , \tag{13}$$

where t_d is a cut-off time, $G_{s,ij}(r)$ is a value of the influence function in steady state, while $G_{t,ij}(r)$ is a transient part of the influence function.

Green's functions are determined individually for each supervised region, and in case of thermal stresses these functions must be determined for each component of the stress tensor σ_{ij}.

An example of Green's function for temperature and stress components at step increase of fluid temperature by 1 °C heating the external surface of a long cylinder is shown in Fig. 6. The calculations were performed with constant heat transfer coefficient $\alpha = 1000$ W/m^2/K and constant material physical properties evaluated at temperature 350 °C. The temperature (Fig. 6a) and stress (Fig. 6b) responses are presented for the cylinder axis and its outer surface heated by steam.

The Green's function for surface temperature, *X_ surf*, initially rapidly increases and reaches nearly 1 after approx. 10^4 s. The temperature at cylinder axis, *X_ cent*, shows some inercy and a delay time of temperature response equal 500 s is seen. After this time the temperature increases at approximately constant rate and after about 4000 s the rate of variation visibly starts to decrease. The cylinder surface response is typical for surface-type sensor, while Green's function at cylinder axis is a response of middle-type sensor. The stress response at both areas is a result of temperature variations: axial and circumferential stresses at cylinder surface are equal to each other and rapidly grow reaching a minimum (compressive stress) and subsequently tend slowly to zero; the stresses at cylinder axis grow more slowly, their maxima are lower than at surface (axial stress is two times higher than circumferential stress) and are tensile stresses (sign +).

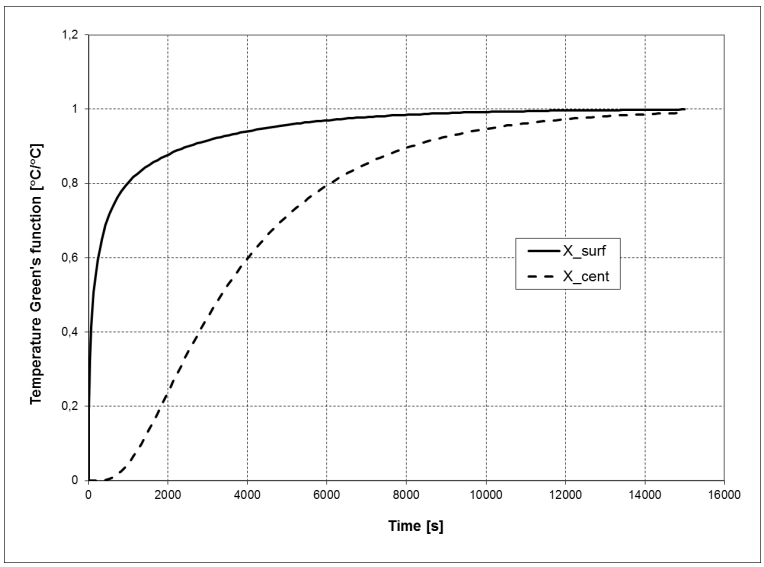

a)

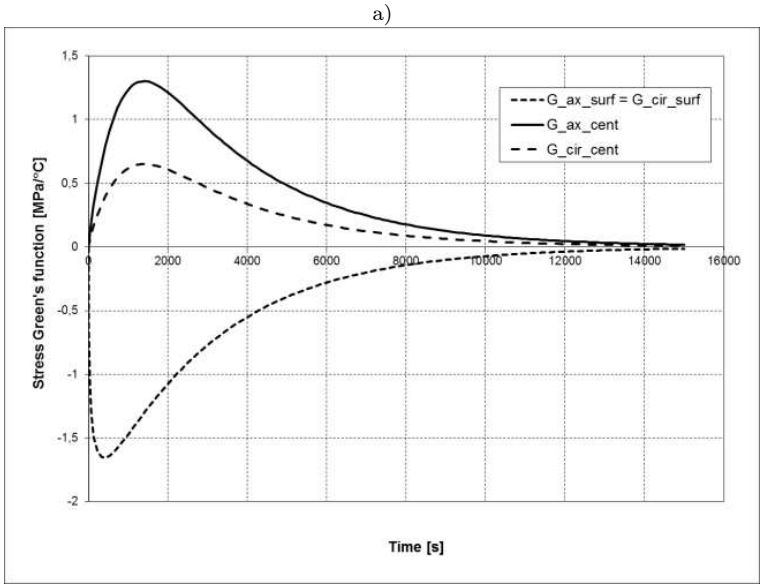

b)

Figure 6: Green's functions for temperature X (a) and stress G (b) for externally heated cylinder.

All stress components within the cylinder tend to zero and a stress-free state is reached after approx. 1.4×10^4 s, which corresponds to the instant when temperature within the whole cylinder is uniform.

4.2 Green's function for temperature dependent material properties and time dependent heat transfer coefficient

The presented in the previous section Green's functions for temperature X and thermal stresses G were determined with constant physical properties and constant heat transfer coefficient α. The physical properties of steel influencing temperature (specific heat, c_p, thermal conductivity, λ) and stress (Young's modulus, E, Poisson's number, ν, thermal expansion coefficient, β) distribution strongly depend on temperature, while heat transfer coefficient α varies with temperature and flow velocity (via the Reynolds number Re). The dependence of these coefficients on temperature and velocity for typical operating conditions of 1CrMoV rotor is shown in Figs. 7 and 8. The heat transfer coefficient in labyrinth seal was calculated using Kapinos *et al.* correlation [33]:

$$\frac{\alpha\cdot d}{\lambda} = 1.125\mathrm{Re}^{0.65}\left(\frac{\delta}{h}\right)^{0.35}\left(\frac{h}{s}\right)^{0.1}\left(\frac{b}{s}\right)^{0.32}, \tag{14}$$

where d is the shaft diameter, δ is seal radial clearance, h is seal channel height, s is the distance between teeth, and b is the teeth width.

Among the considered physical properties the most varying is the specific heat which in the analysed temperature range increases by more than 50%. The largest drop is observed for the Young's modulus which decreases by more than 30%. Heat transfer coefficient depends most on the flow velocity. From the variation of labyrinth seal, a, shown in Fig. 8 it is seen that its value can change even by an order of magnitude. The influence of temperature is smaller and more distinct in the range of higher velocities.

A consequence of the above shown variation of physical properties and heat transfer coefficient is a dependence of Green's function, G, on these parameters. The dependence is illustrated in Fig. 9 showing Green's function variations for axial stress at cylinder surface calculated by finite element method at different temperatures and heat transfer coefficients. Each individual curve corresponds to stress variation determined at constant temperature, $T = const$, and constant heat transfer coefficient, $\alpha = const$. The variation range of these parameters was assumed so as to cover typical operating conditions of 1CrMoV rotors. As it is seen from the plots, the largest effect on the Green's function G is observed for the heat transfer coefficient, which significantly affects the stress maxima, time of

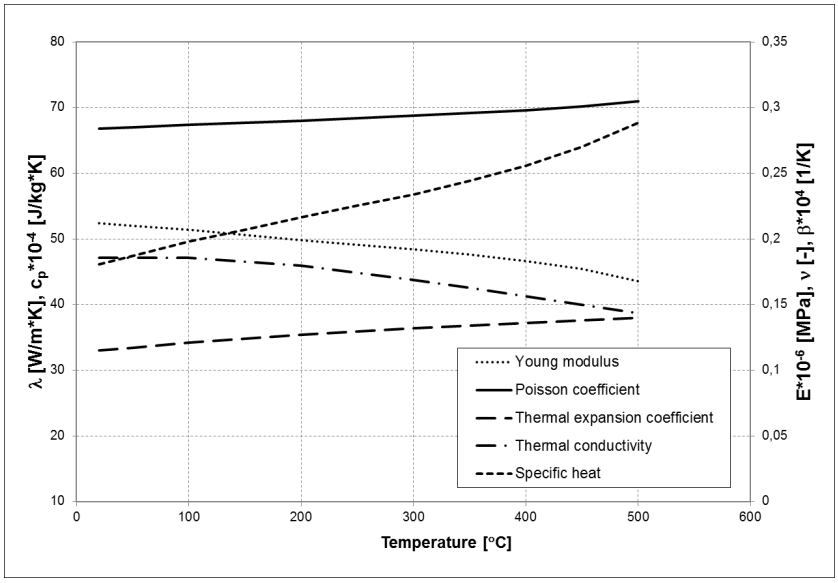

Figure 7: Dependence of typical physical properties of 1CrMoV rotor steel on temperature.

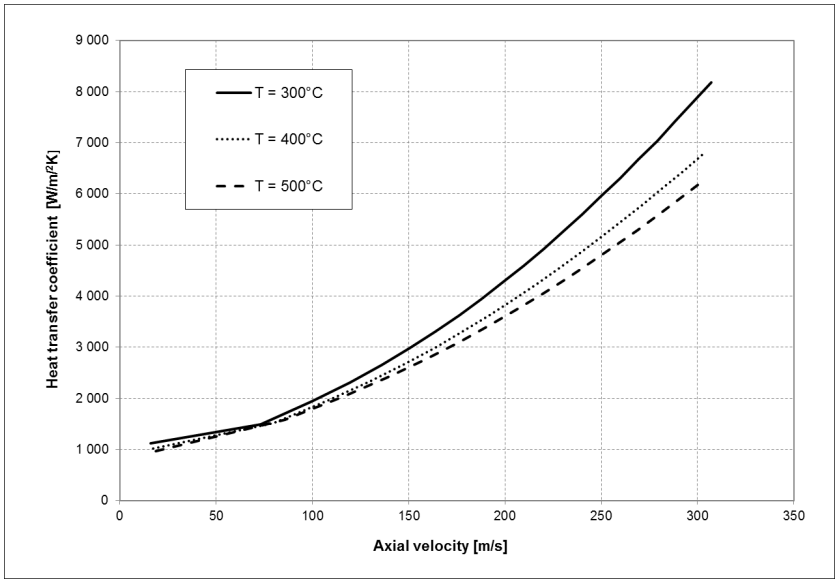

Figure 8: Dependence of heat transfer coefficient on temperature and velocity, accor. Eq.(14).

their occurrence and decay rate. The influence of temperature variation is much smaller and most visible from the instant of maximum stress to the moment of their vanishing.

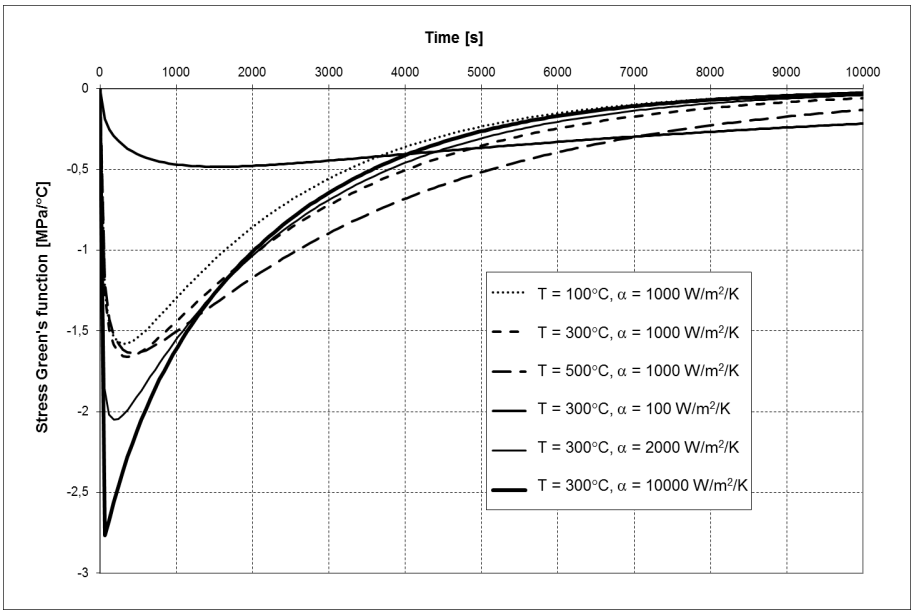

Figure 9: Green's function, G, for axial stress at cylinder surface at various temperatures and heat transfer coefficients.

As a result of so high sensitivity of Green's function, G, to the conditions at which it was determined, a scatter in stress variation calculated using Eq. (13) with different Green's function is observed. Figure 10 presents axial stress variation with time for cylinder surface calculated using the functions presented in Fig. 9. The calculations were performed for the following conditions:

initial conditions:	metal temperature $T_m(0) = 100\,^\circ\mathrm{C}$
	steam temperature $T_s(0) = 200\,^\circ\mathrm{C}$
boundary condition:	steam temperature rate $dT_s/dt = 2\,^\circ\mathrm{C}/\mathrm{min}$

For comparison, also the axial stress variation calculated in three dimensional heat transfer model with the same initial and boundary conditions but with heat transfer coefficient, a, linearly changing with time from 100 to 10000 $\mathrm{W/m^2/K}$ is shown. The heat transfer coefficient was varied until $t = 9000$ s and from this instant remained constant.

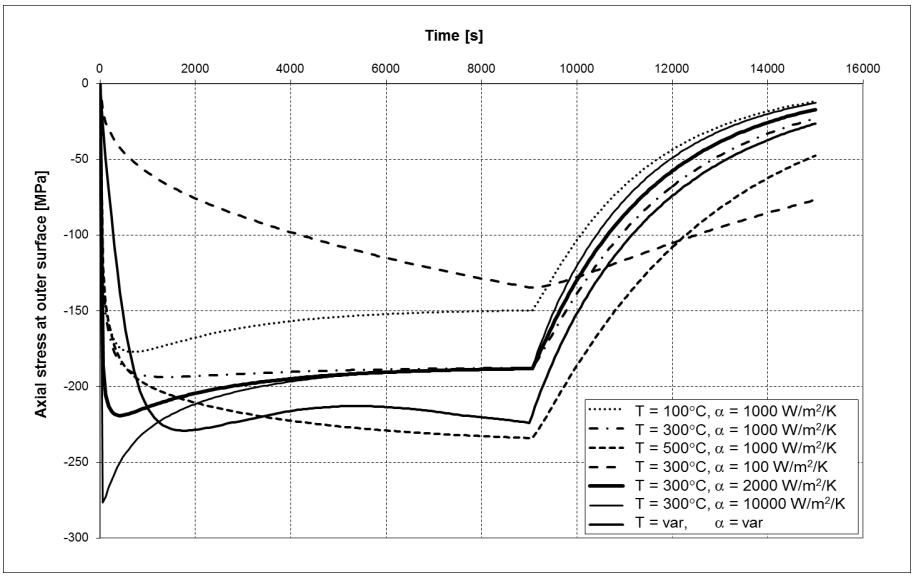

Figure 10: Axial stresses at cylinder surface during heating-up with a rate of 2 °C/min for Green's functions determined at different conditions.

As it is seen from the presented stress variations, the assumption of constant physical properties or constant heat transfer coefficient leads to large errors in calculating thermal stresses at large variations of these parameters. In order to improve the accuracy of thermal stress calculations using Duhamel's integral, Eq. (13), it was proposed to take into account the influence of temperature and heat transfer coefficient on the shape of Green's functions. It was realized by assuming variation in time of the heat transfer coefficient, α, and calculating the equivalent Green's function, G_{eq}, by imposing steam temperature step change from a minimum to a maximum temperature of the element. By imposing such a step change we took into account the variation of material physical properties in the predicted range of operating temperatures. Green's functions for cylinder axial and circumferential stresses calculated in such a way are shown in Fig. 11. The functions were evaluated numerically by assuming, as before, linear variation of the heat transfer coefficient, α, from 100 W/m^2/K to 10000 W/m^2/K in time t = 9000 s and step temperature change from 100 °C to 500 °C. The physical properties of steel were assumed as temperature-dependent according to the curves shown in Fig. 7. The Green's functions calculated in such a way are not qualitatively different compared with those determined at temperature T = 350 °C and heat transfer coefficient α = 10000 W/m^2/K. Due to different parameters at

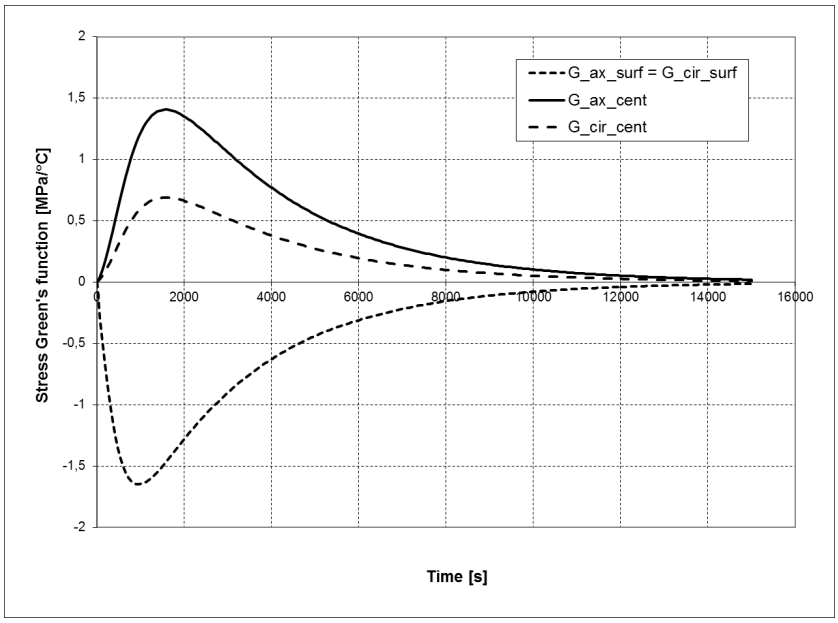

Figure 11: Equivalent Green's function for axial and circumferential stresses in cylinder determined at time-dependent temperature and heat transfer coefficient.

which both sets of functions were determined, small differences in stress maxima and times of their occurrence are seen.

Using the Green's functions shown in Fig. 11, thermal stress calculations were performed for cylinder heating-up at the same conditions as in the previous example and the results are presented in Fig. 12. It is clearly seen that not only qualitative but also very good quantitative agreement between the predictions of Green's function method and nonlinear three dimensional model was achieved.

4.3 Model verification for turbine rotor

The proposed concept of equivalent Green's function, G_{eq}, was validated on an example of a high pressure steam turbine rotor. A cold start-up lasting 240 min was analyzed. The selected example is characterized by a much more complicated geometry and high variability and nonuniformity of thermal boundary conditions resulting in generation of highly non-uniform temperature and stress fields within the rotor. A geometric model of the rotor with a zoomed first blade groove being a critical location is shown in Fig. 13. A variation in time of the turbine mass flow rate, steam temperature and heat transfer coefficient is shown in Fig. 14. All

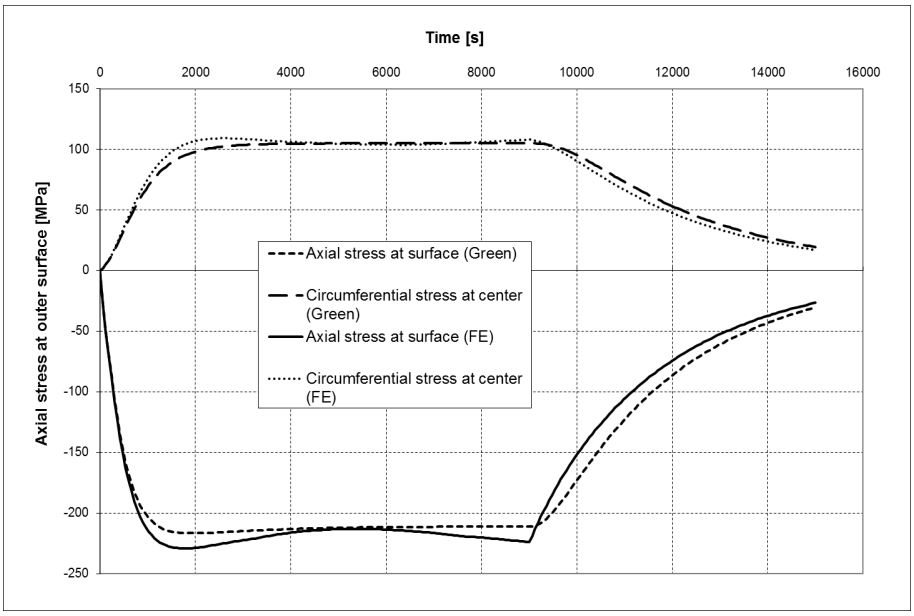

Figure 12: Axial and circumferential stresses in cylinder during heating-up with a rate of 2°C/min calculated using equivalent Green's functions.

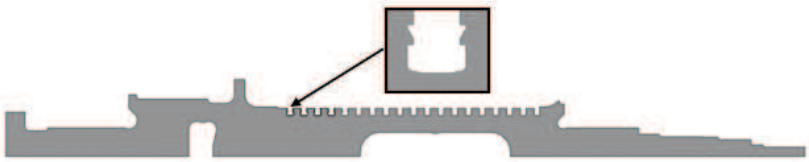

Figure 13: Rotor model with a zoomed first blade groove.

quantities are related to its values at nominal conditions.

Temperature and stress calculations were performed by means of a 3D model of heat and momentum transport using the rotor axisymmetry. In the simulations, temperature-dependent material physical properties and time- and space-dependent (in axial direction) heat transfer coefficients on the rotor outer surfaces were used. The rotor blades were not included in the model, and internal surfaces of the blade grooves were assumed as adiabatic. The stress calculations were performed using linear elastic material model. The rotor initial temperature was 100 °C.

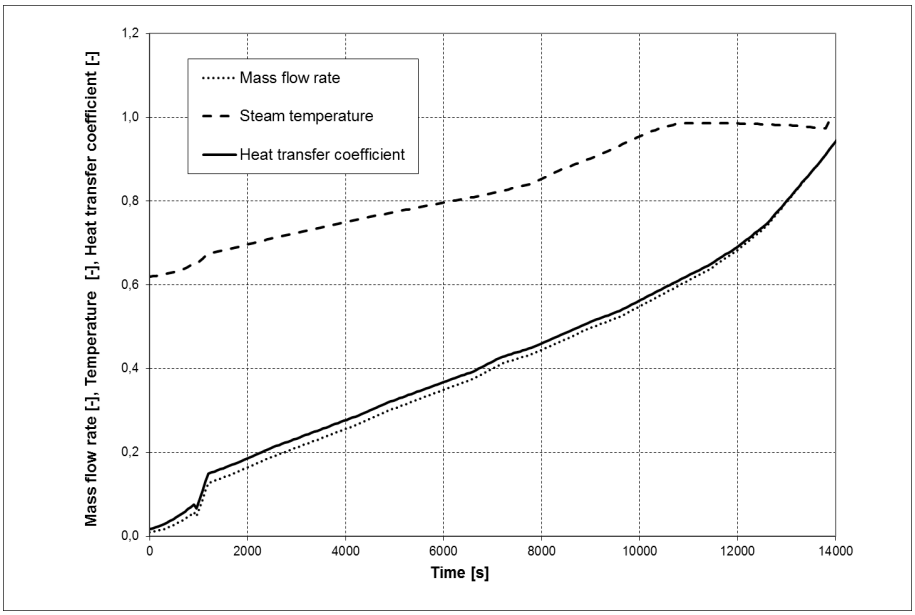

Figure 14: Variation in time of the mass flow rate, steam temperature and heat transfer coefficient.

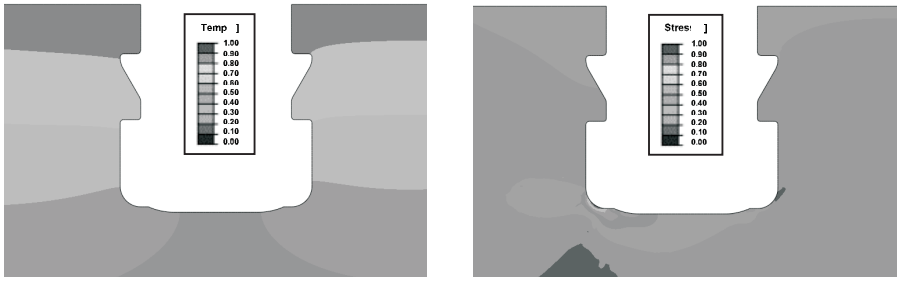

a) b)

Figure 15: Temperature (a) and equivalent Huber-Mises-Hencky stress (b) distribution in first blade groove after 1500 s from the beginning of start-up.

Based on the variation in time of the rotor stress field it was found that the largest stresses are generated at the bottom of the first blade groove. Figure 15 presents the temperature (a) and equivalent Huber-Mises-Hencky stress fields in the region of blade groove after 1500 s from the beginning of start-up. At this instant, a global stress maximum in the rotor during the whole start-up occurred. As it is seen from the temperature distribution, a high radial gradient of tempera-

ture in the groove occurred and temperature difference between the rotor surface and blade groove bottom reached 30% of the surface temperature. In the bottom left corner of the groove, very high stresses were generated at this instant and they were highly concentrated at his point. The stress field away from this region was more uniform, and the stress values much lower than in the concentration area – on the level of 30% of maximum stress.

Next, the equivalent Green's functions for the point where stress maximum occurred were determined. The form of these functions for individual stress components is shown in Fig. 16. It is clearly seen that all Green's functions are negative, which means that with temperature increase all components of the thermal stress tensor will be negative, so at the groove bottom a state of multiaxial compression will persist.

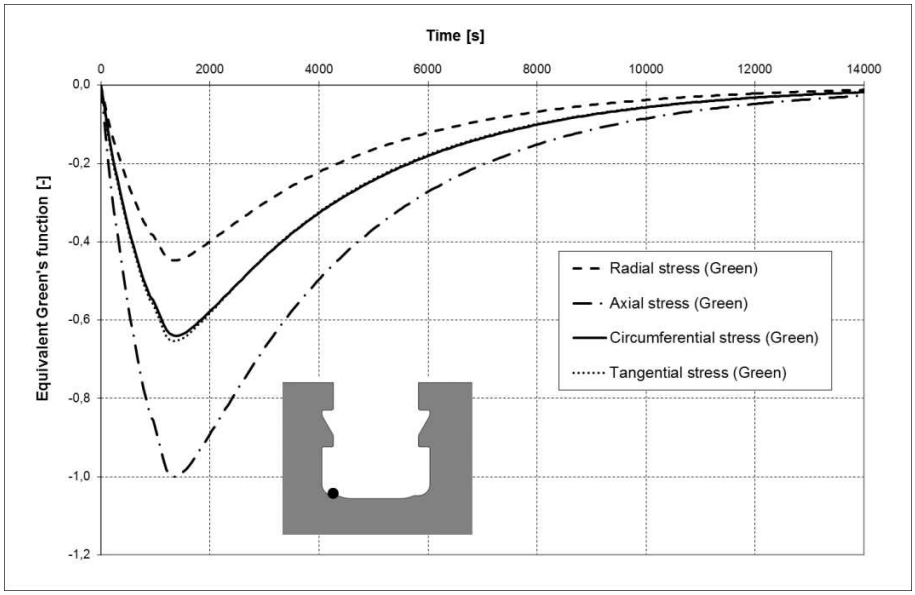

Figure 16: Equivalent Green's functions for stresses at blade groove bottom (red point).

Employing the equivalent Green's functions presented in Fig. 16, stress calculations were performed for the considered start-up using Duhamel's integral, Eq. (13), and the results were compared with the predictions of 3D model. Comparison of the variation of radial and circumferential stress components as well as Huber-Mises-Hencky stress calculated by two methods is shown in Fig. 17. It is seen from the stress curves that a very good accuracy was achieved both for the stress components and the equivalent stress. The stress curves coincide with each

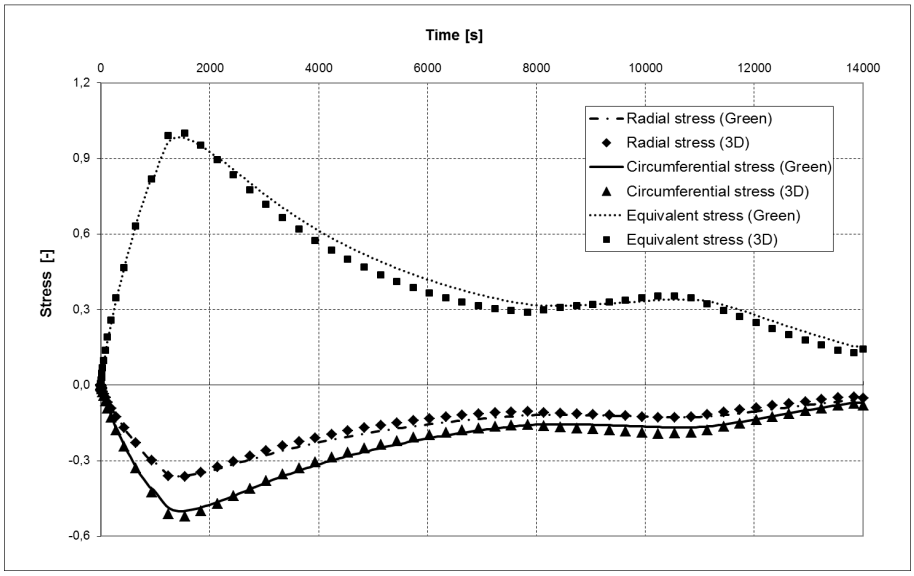

Figure 17: Variation of the groove stresses during cold start-up calculated using equivalent Green's functions (lines) and 3D model (points).

other both during stress increase and decrease; also the local stress maxima and minima occurring after 1500 and 10500 s correspond very well.

The achieved accuracy of blade groove stress predictions for this particular geometry and operating parameters provides a basis for expecting a general capability of equivalent Green's functions and Duhamel's integral to accurately predict thermal stress evolution in steam turbine rotors. Further investigations would be required in order to confirm a potential general applicability of this approach to different designs and operating conditions. The use of equivalent Geens's functions in Duhamel's integral which were evaluated by solving a problem with nonlinear boundary conditions and variable physical properties can provide an accurate solution for thermal stresses, despite the fact that the integral was derived for linear problems (i.e., constant heat transfer coefficient and physical properties).

For online monitoring and control of thermal stresses in steam turbine rotors during start-ups, it is necessary to use Green's functions determined for thermoflow conditions typical for cold, warm and hot starts and use in the stress model different Green's functions, depending on the start-up type.

5 Conclusions

The paper presented a methodology of online thermal stress calculation and control in steam turbine rotors. The main elements of the proposed methodology are: thermodynamic model allowing for calculating steam temperature at critical locations and rotor thermal stress model.

For calculating thermal stresses, steam temperature is used as a leading input signal which is calculated on the basis of thermodynamic model of the turbine inlet part. In such a case, it is not necessary to install a steam temperature measurement as the model is based on the turbo-set standard measurements. A model of the control stage with four nozzle sectors capable of calculating transient steam temperature downstream the stage for arbitrary openings of the control valves is studied. Steam temperature measurements carried out during turbine transient operating conditions and presented here for a warm start-up showed a potential accuracy of the investigated model.

In the rotor thermal stress model, Green's function and Duhamel's integral are used. A crucial effect of the variation of material physical properties and heat transfer coefficient on the shape of Green's function and thermal stress evolution was shown on the example of a simple cylinder representing turbine rotor heated at constant rate. In order to take into account these variations the so-called equivalent Green's function was proposed, which provides a potential for accurate calculation of thermal stresses both for simple geometries and temperature changes (heating-up of cylinder), and for more complicated shapes of real steam turbine rotors (e.g., blade grooves). However, it's general applicability to steam turbine rotors should be confirmed by further investigations. The equivalent Green's functions are valid for given in advance thermo-flow conditions and their applicability to turbines' start-ups is possible thanks to the exact definition at design phase of start-up types and conditions at which they occur.

Received in July 2016

References

[1] Vogt J., Schaaf T., Helbig K.: *Optimizing lifetime consumption and increasing flexibility using enhanced lifetime assessment methods with automated stress calculation from long-term operation data*. In: Proc. ASME Turbo Expo 2013, San Antonio, June 03–07, 2013, GT2013-95068.

[2] Starkloff R., Alobaid F., Karner K., Epple B., Schmitz M., Boehm F.: *Development and validation of a dynamic simulation model for a large coal-fired power plant*. Appl. Therm. Eng. **91**(2015), 496–506.

[3] Otterlee T., Lindsay G.: *Using finite element analysis and thermal stress monitoring to manage turbine defects without mechanical intervention*. Joint Power Generation Conference **3**(1995), 295–299.

[4] Pahl G., Reitze W., Salm M.: *Monitoring temperature changes in steam turbines*. The Brown Boveri Rev. **51**(1964), 3, 165–175.

[5] Busse L.: *Anfahrsonde*. BBC-Studie HTGD51147, 1973.

[6] Dawson R.: *Monitoring and control of thermal stresses and component life expenditure in steam turbine*. Proc. Int. Conf. on Modern Power Stations, AIM, Liege 1989.

[7] Sindelar R.: *Control of the level of heat stress of the steam turbine metal during start-up and load changes*. Skoda Rev. **4**(1972), 19–30.

[8] Lausterer G.K., Franke J., Eitelberg E.: *Mathematical modeling of a steam generator. Digital computer applications to process control*. Proc 6th IFAC/IFIP Int. Conf., Duesseldorf 1980.

[9] Lausterer G.K.: *On-line thermal stress monitoring using mathematical models*. Control Eng. Pract. **5**(1997), 1, 85–90.

[10] Ehrsam A.: *Steam turbines for solar thermal applications*. Proc of ASME Turbo Expo, Vancouver 2011, GT2011–46955.

[11] Sindelar R., Toewe W.: *TENSOMAX — A retrofit thermal stress monitoring system for steam turbine*. VGB Power Tech. **1**(2000), 60–62.

[12] Rusin A., Łukowicz H., Lipka M., Banaszkiewicz M., Radulski W.: *Continuous control and optimisation of thermal stresses in the process of turbine start-up*. Proc. 6th Int. Cong. on Thermal Stresses, Vienna, 26–29 May 2005.

[13] Stevens G.L., Gerber D.A., Rosinski S.T.: *Latest advances in fatigue monitoring technology using EPRI's FatiguePro software*. SMIRT 1999, 15.

[14] Greisbach T.J., Riccardella P.C., Gosselin S.R.: *Application of fatigue monitoring to the evaluation of pressurizer surge lines*. Nucl. Eng. Des. **129**(1991), 163–176.

[15] Kuo A.Y., Tang S.S., Riccardella P.C.: *An on-line fatigue monitoring system for power plants: Part I – direct calculation of transient peak stress through transfer matrices and Green's functions*. In: Proc. 1986 pressure vessels and piping conference and exhibition, PVP, ASME, Chicago, II, **112**(1986), 25–32.

[16] Kiss E., Ranganath S.: *On-line monitoring to assure structural integrity of nuclear reactor components*. Int. J. Pres. Ves. Piping **34**(1988), 3–15.

[17] Heliot J., Fritz R.: *Framatome operating transients monitoring system used for equipment mechanical surveillance*. Int. J. Pres. Ves. Piping **40**(1989), 247–258.

[18] Aufort P., Bomont G., Chau T.H., Fournier I., Morilhat P., Souchois T., Cordier G.: *On line fatiguemeter: A large experiment in French nuclear plants*. Nucl. Eng. Des. **129**(1991), 177–184.

[19] Taler J., Węglowski B., Zima W., Duda P., Grądziel S., Sobota T., Cebula A., Taler D.: *Computer system for monitoring power boiler operation*. In: Proc. IMechE, Part A: J. Power Energ. **222**(2008), 13–24.

[20] Lee H.Y., Kim J.B., Yoo B.: *Green's function approach for crack propagation problem subjected to high cycle thermal fatigue loading*. Int. J. Pres. Ves. Piping **76**(1999), 487–494.

[21] Dhanuskodi R., Kaliappan R., Suresh S., Anantharaman N., Arunagiri A., Krishnaiah J.: *Artificial neural networks model for predicting wall temperature of supercritical boiler*. Appl. Therm. Eng. **90**(2015), 749–753.

[22] Rusin A., Nowak G., Lipka M.: *Practical algorithms for online stress calculations and heating process control*. J. Therm. Stresses **37**(2014), 11.

[23] Dominiczak K., *Neural networks in thermal stress limiter of steam turbines*. PhD Thesis, IFFM PAS, Gdańsk 2015 (in Polish).

[24] Song G., Kim B., Chang S.: *Fatigue life evaluation for turbine rotor using Green's function*. Proc. Eng **10**(2011), 2292–2297.

[25] Koo G.H., Kwon J.J., Kim W.: *Green's function method with consideration of temperature dependent material properties for fatigue monitoring of nuclear power plants*. Int. J. Pres. Ves. Piping **86**(2009), 187–195.

[26] Botto D., Zucca S., Gola M.M.: *A methodology for on-line calculation of temperature and thermal stress under non-linear boundary conditions*. Int. J. Pres. Ves. Piping **80**(2003), 21–29.

[27] Zhang H.L., Liu S., Xie D., Xiong Y., Yu Y., Zhou Y., Guo R.: *Online fatigue monitoring models with consideration of temperature dependent properties and varying heat transfer coefficients*. Hindwai Publishing Corporation. Science and Technology of Nuclear Installations, 2013, ID 763175.

[28] Taler J.: *Theory and practice of heat transfer processes identification*. Ossolineum, Wrocław 1995 (in Polish).

[29] Lavagnoli S., De Maesschlack C., Paniagua G.: *Uncertainty analysis of adiabatic wall temperature measurements in turbine experiments*. Appl. Therm. Eng. **82**(2015), 170–181.

[30] Badur J., Banaszkiewicz M., Karcz M., Winowiecki M., *Numerical simulation of 3D flow through a control valve*. Int. Conf. SYMKOM'99, Arturówek-Łódź, 5–8 Oct. 1999.

[31] Perycz S.: *Steam and Gas Turbines*. Maszyny Przepływowe Vol. 10, Ossolineaum 1992 (in Polish).

[32] Carslow H.S, Jaeger J.C.: *Conduction of Heat in Solids*. Oxford University Press, Oxford 1959.

[33] Kapinos V.M., Gura L.A.: *Heat transfer in a stepped labyrinth seal*. Teploenergetika **20**(1973), 22–25 (in Russian).